Effect of the Range of Interactions on the Properties of Fluids. Phase Equilibria in Pure Carbon Dioxide, Acetone, Methanol, and Water

Matthias Kettler,[†] Ivo Nezbeda,[*,‡] Ariel A. Chialvo,[§,‡] and Peter T. Cummings[§,||]

Institute of Thermodynamics and Thermal Process Engineering, University of Stuttgart, 70550 Stuttgart, Germany, Department of Chemical Engineering, University of Tennessee, Knoxville, Tennessee 37996-2200, Chemical Sciences Division, High-Temperature Aqueous Chemistry Group, Oak Ridge National Laboratory, Oak Ridge, Tennessee 37831-6110, and Department of Chemical Engineering, Chemistry, and Computer Science, University of Tennessee, Knoxville, Tennessee 37996-2200

Received: January 16, 2002; In Final Form: April 23, 2002

The effect of the long-range Coulombic interactions on the vapor−liquid equilibria properties of polar and associating fluids has been investigated, by considering typical representatives of these classes of fluids, namely, carbon dioxide, acetone, methanol, and water, defined by realistic intermolecular pair potential models. Using the same decomposition of realistic potential models into a short-range part and a residual part as in previous papers [Kolafa, J.; Nezbeda, I. *Mol. Phys.* **2000**, *98*, 1505−1520. Kolafa, J.; Nezbeda, I.; Lısal, M. *Mol. Phys.* **2001**, *99*, 1751−1764], we carried out Gibbs ensemble simulations on both the full and short-range models to determine the thermodynamic properties of the considered compounds along the vapor−liquid coexistence curve. In addition, we also considered methanol in two homogeneous phases, liquid and supercritical, to determine its structure and thermodynamic properties. We have found that the long-range interactions affect all considered properties only marginally and that the short-range system provides a reasonably accurate and reliable zeroth-order approximation. A simple theoretical analysis has also been made to explain and estimate the effect of the long-range interactions on the thermodynamic properties both in the homogeneous phase and at phase equilibrium.

1. Introduction

To find a relation between the observed properties of fluids and the intermolecular interactions acting between their molecules is one of the most important goals of statistical mechanics. Knowledge of such relations helps us not only to understand and predict the properties of fluids, but also makes it possible to develop simple model Hamiltonians (simple models) upon which a theory, and hence workable equations, may be developed. As a typical example consider the various hard-body fluid models, whose origin lies in the recognition that the *structure* of normal (i.e., nonpolar) fluids is determined primarily by strong short-range repulsive interactions.[1]

However, the concept of a simple decomposition of the total pair potential into a repulsive part and an attractive part is not generally thought to be applicable to strongly polar and associating fluids. These fluids are characterized by the presence of the long-range Coulombic interactions which have been believed to be the main contributing factor to their properties. Consequently, these interactions have explicitly been incorporated into simple models designed to capture the essence of physics of polar of associating fluids.[2] Although the theory for such models has reached remarkable results,[3−6] their application to real fluids is rather cumbersome and in the case of associating fluids it encounters fundamental difficulties.

Following the idea that it is rather the range of interactions which matters more than the interaction itself,[7] recently we have investigated in detail the effect of the long- and short-range forces on the structure and thermodynamic properties of nonsimple fluids.[8−11] We have considered three classes of fluids—quadrupolar, dipolar, and associating—and a typical representative within each class—carbon dioxide for the first class, acetone for the second, and water for the third. Starting from realistic Hamiltonians, we constructed short-range models [see eq 5 below], and surprisingly, we found that the long-range Coulombic interactions play, in fact, only a marginal role. The conclusions which can be drawn from these investigations can be summarized as follows:

1. In general, in all cases the effect of the long-range forces on the spatial arrangement of the molecules is very small. Specifically, the structure of the realistic fluids and their short-range counterparts, described by the set of the site−site correlation functions, is very similar (nearly identical).

2. As a consequence of finding (1), the thermodynamic properties of the realistic fluids are very well estimated by those of the short-range models: the internal energy of the short-range models accounts for at least 95% of the total internal energy of the full realistic fluids.

3. The long-range forces affect only details of the orientational correlations and hence, to a certain extent, also pressure. However, integral quantities, such as, e.g., the dielectric constant, remain unaffected.

All above findings are important from the theoretical point of view because they open the possibility of developing a fast

* To whom correspondence should be addressed. E-mail: IvoNez@icpf.cas.cz. On leave of absence from E. Hála Laboratory of Thermodynamics, Academy of Sciences, 165 02 Prague 6, and Department of Physics, Purkyně University, 496 00 Ústı n. Lab., Czech Republic.

† Institute of Thermodynamics and Thermal Process Engineering.

‡ Department of Chemical Engineering.

§ Chemical Sciences Division.

|| Department of Chemical Engineering, Chemistry, and Computer Science.

10.1021/jp020139r CCC: $22.00
Published on Web 07/10/2002

converging perturbation expansion about a short-range reference with the long-range Coulombic interactions treated as a perturbation only.[7,10,12] The feasibility of this approach has been demonstrated recently by deriving a molecular-based equation of state for water.[12] From the practical point of view, the immediate question which arises is to what extent some important properties, such as, e.g., phase equilibria, are affected by the long-range interactions in general. This problem has attracted a good deal of attention, particularly among the chemical engineering community, with the conclusion that the long-range interactions do play a significant role with well detectable trends as these forces increase.[13,14] These claims, obtained only by speculative arguments, are apparently in conflict with the above summarized findings for the homogeneous phase and thus deserves deeper attention. It is the aim of this paper to address this problem by investigating the vapor−liquid equilibria in typical polar and associating fluids: carbon dioxide, acetone, methanol, and water.

For carbon dioxide, acetone, and water we make use of the results of our previous studies[8,9,11] and use the investigated short-range models directly in the Gibbs ensemble (GE) simulations to determine the vapor−liquid equilibria (VLE) and thermodynamic properties along the coexistence curve. Simultaneously, we consider also the full realistic potentials at the same state conditions for comparison. The available literature VLE data for the full potential models are used to check the correctness of the present calculations. In addition to the above three substances, we have included also methanol in our investigations. Methanol falls into the category of associating fluids with a slightly weaker hydrogen bonding in comparison with water and complements therefore the set of considered liquids of different strength and importance of the Coulombic interactions. It is also an important industrial compound used in variety of technologies and has thus attracted a good deal of attention. To find a proper range of the short-range model, we first carried out a number of preliminary simulations on methanol in the homogeneous phase.

After the basic definitions and computational details are summarized in the following section, we present and discuss the results in Section 3. In addition to the simulation results, we have attempted also to carry out a simple theoretical analysis in order to estimate errors in the internal energy, pressure, and the location of the critical point resulting from the neglect of the long-range interactions.

2. Basic Definitions and Computational Details

To describe interactions between molecules of associating and polar fluids in a realistic manner, we use effective pairwise intermolecular potential models. These models assume a rigid monomer with interaction sites located on the nuclei; for hydrocarbons the CH_n groups are treated as united atoms centered on the carbons. The sites are the origin of the Lennard-Jones (LJ) and Coulombic interactions and the interactions between the molecules are represented by site−site potentials. The total interaction energy between a pair of molecules is thus given by

$$u(1,2) \equiv u(R_{12}, \Omega_1, \Omega_2) = \sum_{i\in\{1\}}\sum_{j\in\{2\}}\left\{4\epsilon_{ij}\left[\left(\frac{\sigma_{ij}}{r_{ij}}\right)^{12} - \left(\frac{\sigma_{ij}}{r_{ij}}\right)^{6}\right] + \frac{q_i q_j}{r_{ij}}\right\} = u_{LJ}(1,2) + u_{coul}(1,2) \quad (1)$$

where the set (R_{12}, Ω_i) defines, respectively, the mutual position and orientation of a pair of molecules, r_{ij} denotes the $i-j$ site−site separation, q_i are partial charges, and ϵ_{ij} and σ_{ij} are the pair LJ parameters.

TABLE 1: Lennard-Jones Parameters ϵ_i and σ_i, Partial Charges q_i, and Geometries of the Used Potential Models

atom	ϵ/k_B [K]	σ [Å]	q [e]	geometry
		Carbon Dioxide[18]		
C	28.999	2.785	+0.6645	O−C: 1.163 Å
O	82.997	3.064	−0.33225	O−C−O: 180°
		Acetone[17]		
C	52.84	3.75	+0.566	C−O: 1.223 Å
O	105.68	2.96	−0.502	CH_3−C: 1.572 Å
CH_3	85.00	3.88	−0.032	CH_3−O: 2.443 Å
		Ethanol[16]		
O	85.546821	3.070	−0.700	O−H: 0.945 Å
H	0.0	0.0	0.435	CH_3−O: 1.430 Å
CH_3	104.16583	3.775	0.265	CH_3−O−H: 108.5°
		Water[15]		
O	78.08	3.1535	0.0	O−H: 0.9572 Å
H	0.0	0.0	+0.52	H−O−H: 104.5°
M-site	0.0	0.0	−1.04	O−M: 0.15 Å along the H−O−H bisector

Specifically, for water we use the TIP4P potential,[15] for methanol the OPLS model of Jorgensen,[16] for acetone the model studied by Jedlovszky and Pálinkás,[17] and for carbon dioxide we use Harris-Yung's EPM2 model.[18] The geometry of all models is defined in Table 1 where the potential parameters are given as well.

Whereas the geometric mean is used, as a rule, for the energy to define the cross interactions between the LJ sites of all compounds,

$$\epsilon_{ij} = (\epsilon_{ii}\epsilon_{jj})^{1/2} \quad (2)$$

it has also been used for σ's of methanol and carbon dioxide,

$$\sigma_{ij} = (\sigma_{ii}\sigma_{jj})^{1/2} \quad (3)$$

For acetone, the usual arithmetic mean for σ's is used,

$$\sigma_{ij} = \frac{\sigma_{ii} + \sigma_{jj}}{2} \quad (4)$$

To investigate the effect of the range of interactions on the structure of fluids, we construct a short-range potential, u_{sr}, by cutting off smoothly all the long-range interactions,[8]

$$u_{sr}(1,2) = u(1,2) - S(r_{CC};R_1,R_2)u_{coul}(1,2) = u_{LJ}(r_{CC}) + [1 - S(r_{CC};R_1,R_2)]u_{coul}(1,2) \quad (5)$$

where S is a switch function,

$$S(r;R_1,R_2) = \begin{cases} 0 & \text{for } r < R_1, \\ (r-R_1)^2(3R_2 - R_1 - 2r)/(R_2 - R_1)^3 & \text{for } R_1 < r < R_2, \\ 1 & \text{for } r > R_2, \end{cases} \quad (6)$$

R_1 and R_2 are its parameters defining the transition range, and r_{CC} is the separation between the reference sites. We denote this short-range potential as (R_1, R_2). For the reference site we choose oxygen in the case of methanol and water, and carbon for carbon dioxide and acetone.

We used the standard Monte Carlo simulations in an NVT Gibbs ensemble (GE)[19] to study phase equilibria properties. With the exception of the highest temperature, for which we used 600−700 particles, at all other conditions were carried out the simulations with $N = 512$ particles. The boxes were set up so that the number of particles in the vapor box varied between 50 and 150 over the entire temperature range, and the box length was always greater than twice the cutoff distance. Simulations were performed in cycles, each circle consisting of N trial translations, N trial rotations, 1 trial volume change, and $10 \times N$ transfer moves. The moves were selected at random and the acceptance ratio for the trial moves was adjusted to about 1:3. In an attempt to improve efficiency of the simulation at high densities, for methanol at $T = 360$ K, we also used the orientational−insertion bias.[20] However, with regard to the number of successful insertions per CPU time, the method was found comparable with the standard GE sampling and therefore was not considered further. After equilibration period, about $(5-10) \times 10^5$ cycles were used to collect the appropriate histograms and estimate simulation errors by the block method.[21]

The long-range interactions were treated by means of the reaction field method.[22] Thus, the long-range corrections were incorporated into the pair interactions whose Coulombic part assumed then the form

$$u_{\mathrm{coul}}(1,2) = \sum_{i\in\{1\}} \sum_{\in\{2\}j} \frac{q_i q_j}{r_{ij}} \left[1 + \frac{\epsilon_{\mathrm{RF}} - 1}{2\epsilon_{\mathrm{RF}} + 1} \left(\frac{r_{ij}}{R_{\mathrm{cut}}} \right)^3 \right] \qquad (7)$$

with the reaction field dielectric constant ϵ_{RF} set to infinity (metal-like boundary conditions). R_{cut} is the cutoff radius beyond which all interactions are set to zero. To maintain electrical neutrality of the molecules, this cutoff radius refers to the reference points within the molecules rather than to the individual sites. We used the same cutoff radius for the LJ interactions and applied the usual long-range correction.

Since methanol has not been considered in our previous studies, it is important to study its properties away from the phase equilibrium region as well. We used molecular dynamics (MD) simulations with 500 molecules at isothermal-isochoric conditions using the Nosé thermostat.[23] The Newton−Euler equations of motion were integrated using the fifth and fourth order Gears' predictor−corrector[24] for the translational and rotational degrees of freedom, respectively, with a time step of 1.0 fs. The rigid body orientations were described by Evans−Murad quaternion formalism[25] and the long-ranged electrostatic interactions were also handled by the reaction field with the metal-like boundary conditions as described above. Typical simulation runs span the interval of 200 ps following the 30 ps equilibration period. The desired output of the simulations were the internal energy and pressure, as well as the site−site correlation functions. To obtain the latter quantities, we followed the method described in detail in our previous papers[8,9,11] and refer therefore the reader to these papers for the appropriate definitions and all necessary computational details.

3. Results and Discussion

To maintain compatibility with previously published GE data for the full realistic models, generally we followed the specific technical details used to produce these data. Thus, for carbon dioxide the potential cutoff was set to $3.6\sigma_{\mathrm{CC}}$,[18] and for acetone to $5.07\sigma_{\mathrm{CC}}$.[17] For water and methanol we followed Lısal et al.[26] who used the half length of the simulation box as cutoff. Since in GE simulations the box length varies, we used the fixed value which was the largest (and the same) possible cutoff in both boxes under the constrain that it never exceeds the half-length of the box.

TABLE 2: Parameters of the Switch Functions

	carbon dioxide	acetone	methanol	water
R_1 [Å]	4.0	6.6	5.7	4.0
R_2 [Å]	6.0	8.0	7.7	6.0

Concerning the short-range models, the switching range was well established in previous studies for carbon dioxide, acetone, and water[11,9] and the parameters R_1 and R_2 are given in Table 2. For methanol we first carried out MD simulations in the homogeneous phase and these results are discussed in the following subsection. The resulting parameters R_1 and R_2 are also given in Table 2.

3.1. Structure and Thermodynamics of Methanol. The considered (effective) model of methanol pictures its molecule as a nonlinear triatomics with the dipole moment $\mu_{\mathrm{mod}} = 2.2$ D, which is significantly greater than the experimental value $\mu_{\mathrm{exp}} = 1.7$ D[27] in order to account for a rather large polarizibility ($\alpha \approx 3.3$ Å^3). For the dimer the global internal energy is $U = 28.45$ kJ/mol for the configuration with a linear hydrogen bond and the O−O separation $=2.73$ Å.[16]

Two sets of simulations were carried out, one for the short-range model and the other for the full-range model. For each model two sets of simulations were carried out along two different thermodynamic paths: one along the $\rho = 761.9$ kg/m^3 isochore over the temperature range $298 \le T \le 548$ K, the other along the $T = 548$ K isotherm over the density range $61.9 \le \rho \le 961.9$ kg/m^3. For each set of simulations we characterized the behavior of the considered models in terms of the pressure, configurational internal energy, and site−site pair correlation functions with the goal of finding the range of the most important intermolecular interactions (i.e., the range which affects the fluid properties most).

Following the known results for water,[9] we started first with the set $(R_1, R_2) = (4, 6)$[Å] for which we found significant discrepancies, particularly for g_{OO} and g_{OH} correlation functions, see Figure 1. We then tried the range $(R_1, R_2) = (4.7, 6.7)$[Å] but the discrepancies (though smaller) still persisted. Finally we settled with $(R_1, R_2) = (5.7, 7.7)$[Å] for which the predicted structure of the short-range model is indistinguishable from that for the full potential. These results confirm thus the previous findings for acetone and water, namely, that the short-range model should cover the first coordination shell. An analysis of the results for the full model showed that the minimum on g_{CC} is located, approximately, between 5.5 Å and 6 Å.

In Figures 2 and 3 we display, respectively, the resulting structures in terms of the same four site−site pair correlation functions as in Figure 1 for four temperatures along the isochore $\rho = 761.9$ kg/m^3, and for four densities along the isotherm $T = 548$ K.

According to Figure 2, as the temperature increases along the isochore, the peaks get lower and wider as we might expect. Note that while the location of the first peaks changes only slightly (usually less than 0.05 Å shift to smaller distance with temperature, except for the g_{OH}), the location of the second peaks shift more pronouncedly (more than 0.1 Å in the same directions as the corresponding first peaks). In contrast, Figure 3 shows that the isothermal-density effect is more dramatic, especially for g_{CC}, where the first 1.0 Å shift to the left as the density increases from 61.9 to 961.9 kg/m^3 (a similar shift is also observed in the location of the second peak). The remaining g's exhibit very weak density effect on the location of the peaks

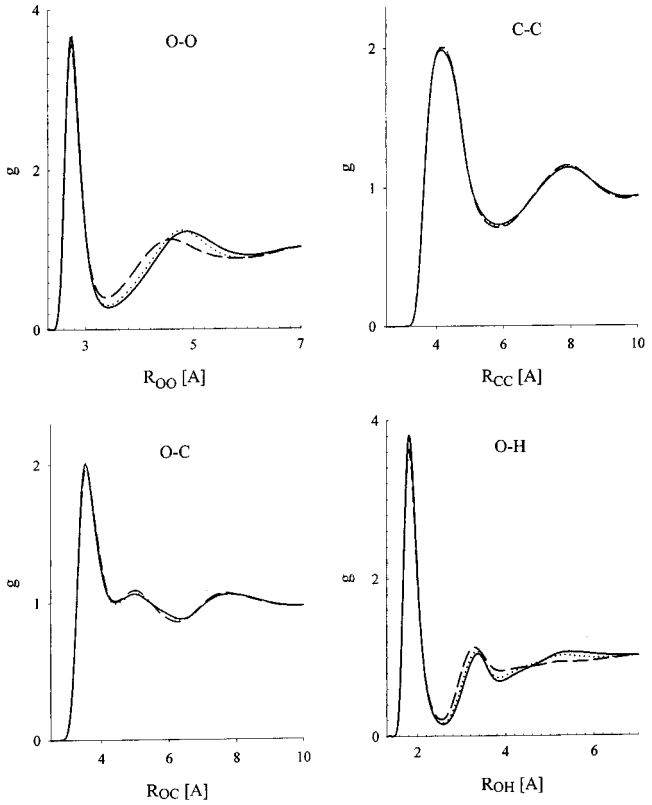

Figure 1. Site-site correlation functions of methanol at density $\rho = 761.9$ kg/m^3 and temperature $T = 298$ K as a function of the switch range (R_1, R_2): dashed line (4, 6)[Å], dotted line (4.7, 6.7)[Å], full line (5.7, 7.7)[Å].

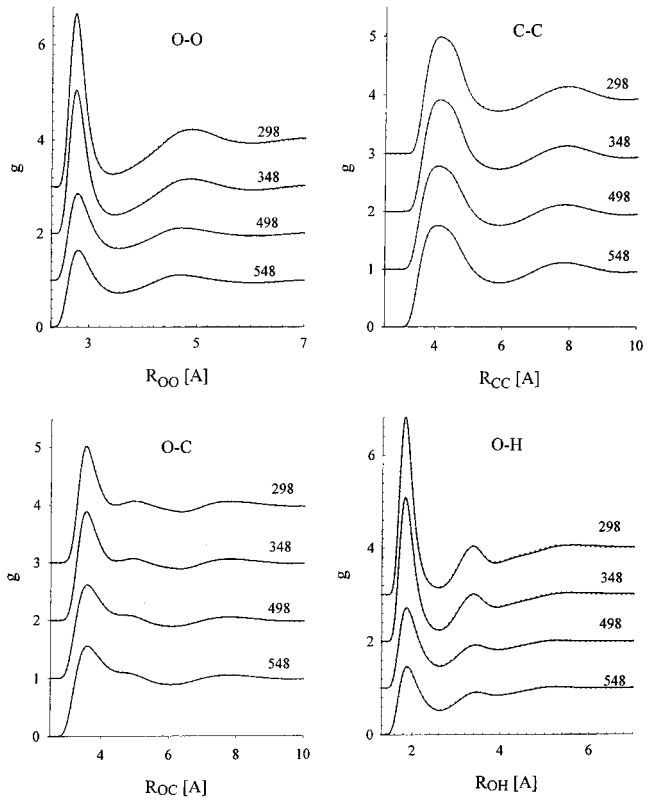

Figure 2. Site-site correlation functions of the short-range (dotted line) and full models (solid line) of methanol for different temperatures (labels at curves) at density $\rho = 761.9$ kg/m^3.

(usually these shifts are to shorter distances as the density increase, i.e., as we might expect). The other obvious density effect on the structure is the formation of stronger coordination shells with increasing density.

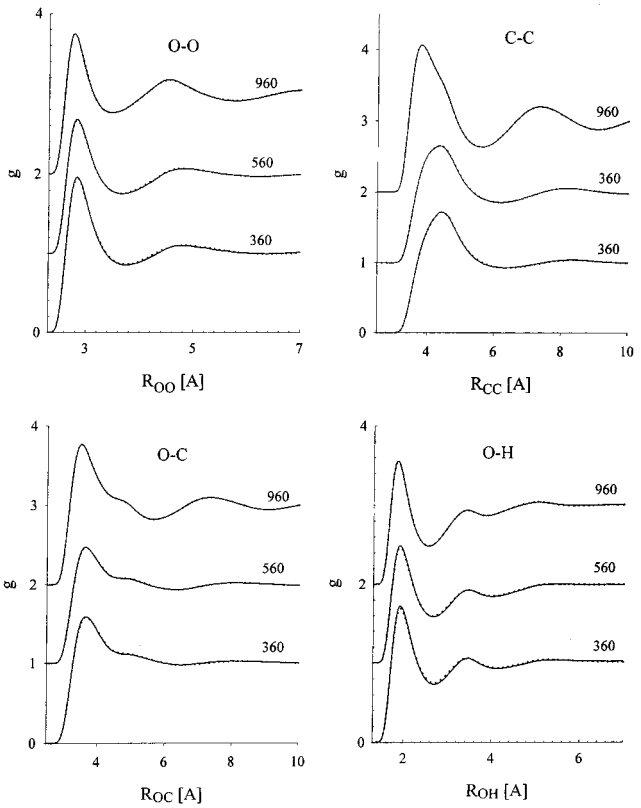

Figure 3. The same as Figure 2 for the different densities along the supercritical isotherm $T = 548$ K.

The first peaks of g_{OO} and g_{OH} are usually (loosely) taken as the manifestation of the hydrogen bond structure. Along the 761.9 kg/m^3 isochore the hydrogen-bond structure does not exhibit a noticeable change, in that the corresponding coordination numbers $\mathcal{N}_{OO}$ and $\mathcal{N}_{OH}$ (defined by the first valley of the corresponding g's) are 1.99 and 1.95 for $T = 298$ K, and 1.90 and 1.55 at $T = 548$ K. The clear expected but small decrease of $\mathcal{N}_{OH}$ with temperature is also accompanied by an increase of the corresponding $\mathcal{N}_{HH}$ from 4.5 to 4.8. The picture is rather different for the density effect along the supercritical temperature $T = 548$ K. In this case the $\mathcal{N}_{OO}$, $\mathcal{N}_{OH}$, and $\mathcal{N}_{HH}$ increase from (0.42, 0.30, 1.15) at 61.9 kg/m^3 to (2.8, 2.2, 2.05) at 961.9 kg/m^3, i.e., the density increase induces a strengthening of the hydrogen bond structure (in the loose sense we mentioned above).

In Figures 4 and 5 we compare the internal energy and pressure of the short-range and full models at different densities and temperatures. As it is seen, the results are in full agreement with previous findings summarized in the Introduction. The internal energies in the dense phase along the isochore do not differ by more than 4% for the entire temperature range considered, and the same holds true also for the internal energy along the supercritical isotherm. In the latter case the results begin even to agree within the simulation error bars with decreasing density. A similar trend is observed also for the energies along the isochore. In all cases the internal energy of the short-range model is greater (smaller in the absolute value) than that of the full model. A similar result with $P_{short} > P_{full}$ holds true for pressure, although differences are evidently somewhat larger, see item (3) in the Introduction.

3.2. Vapor−Liquid Equilibria. In Figures 6−8 we compare the pressure, internal energy, and density of the coexisting vapor

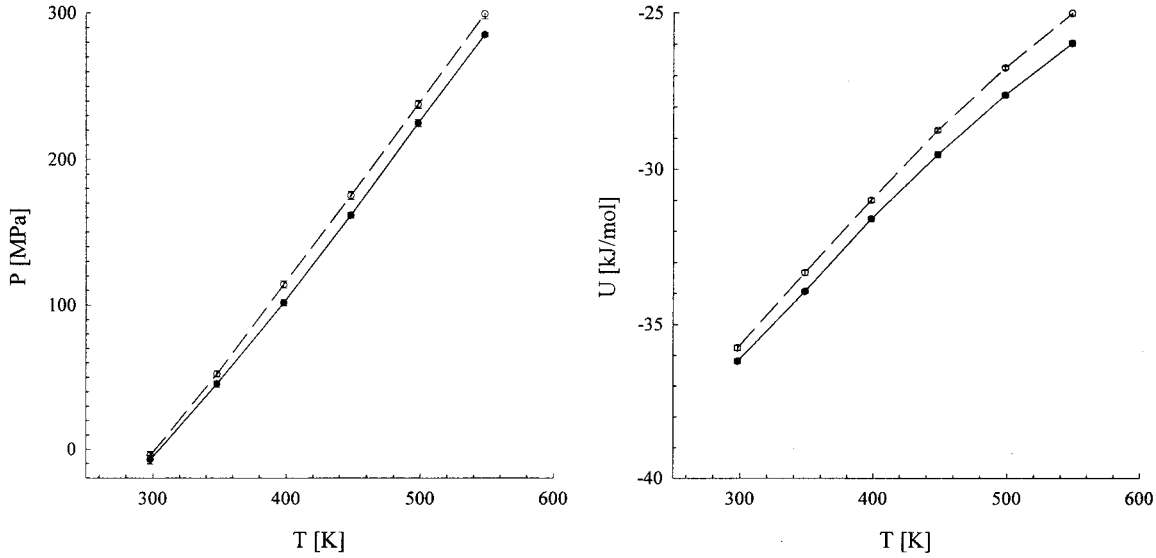

Figure 4. The internal energy U and pressure P of the short-range and full models of methanol for different temperatures at $\rho = 761.9$ kg/m^3. The filled symbols and solid lines are results for the full system; lines are drawn as the guide for eyes.

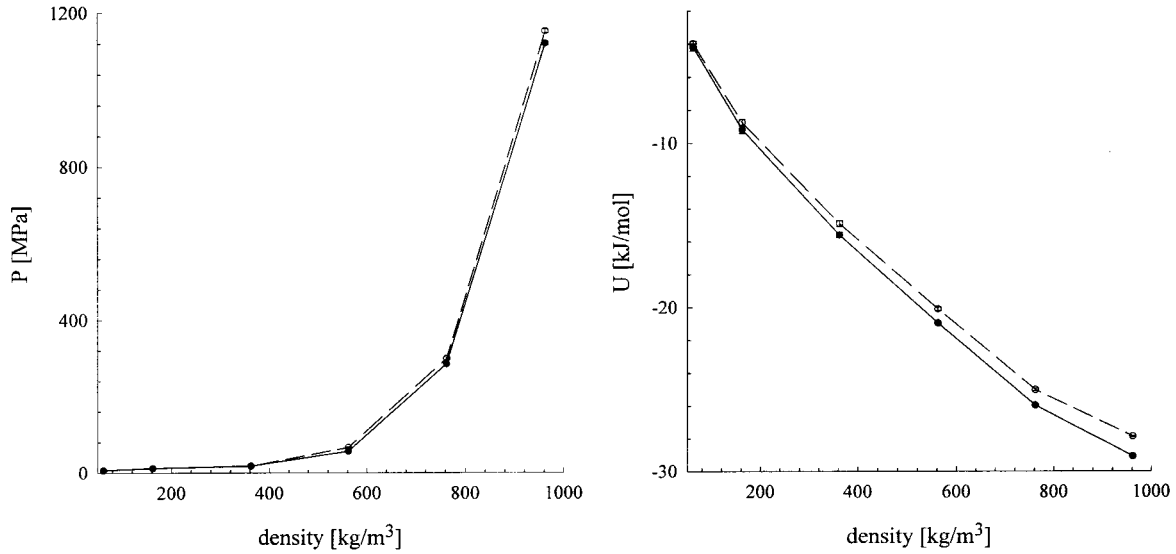

Figure 5. The same as Figure 4 for densities along the supercritical isotherm $T = 548$ K.

and liquid phases of the short-range and full systems for all four compounds.

From the construction of the short-range model, eq 5, it follows that it misses a piece of an attractive interaction present in the full model. Intuitively one may thus expect an increase in pressure in the short-range system and this is really true. Along the entire coexistence curve it holds: $P_{full}(T) < P_{short}(T)$ as for the homogeneous phase discussed above. The discrepancy is very small, particularly at low temperatures, and it is within the combined simulation errors over the entire temperature range for carbon dioxide, acetone, and methanol. A larger discrepancy is found only for water at elevated and high temperatures.

No such simple intuitive arguments can however be applied to the temperature dependence of the internal energy at orthobaric densities, Figure 7. In general, we find the same result as for the homogeneous phase: the difference in the internal energy between the full and short-range systems does not exceed 4% for all compounds and the entire coexistence range. A more detailed analysis then reveals that (i) the internal energies for the full and short-range models for all compounds in the gas-phase agree within the simulation errors, (ii) for all compounds but acetone, the internal energies for the full and short-range models in the liquid-phase agree within the combined error bars over the entire coexistence range with the exception of the lowest temperature, and (iii) there is no unique inequality between the energies of the full and short-range models in the liquid phase. Whereas for carbon dioxide we have $U_{short} > U_{full}$ as one would expect, for water and acetone we have $U_{short} < U_{full}$.

To understand this behavior, we have to analyze available data for homogeneous phases. As mentioned already above, one would expect the internal energy of the full system to be more negative (greater in the absolute value) compared with that for the short-range model. This is really true but at low densities only. Simulation results for water[10] along low-temperature isotherms in the dense liquid phase show that $U_{short} < U_{full}$ and that this inequality changes sign at supercritical temperatures. Furthermore, the difference between the results for the full and short-range models tends to zero with decreasing density for low-temperature isotherms. The result found for the internal energy of liquid water in coexistence with its vapor is thus consistent with these observations and also explains better

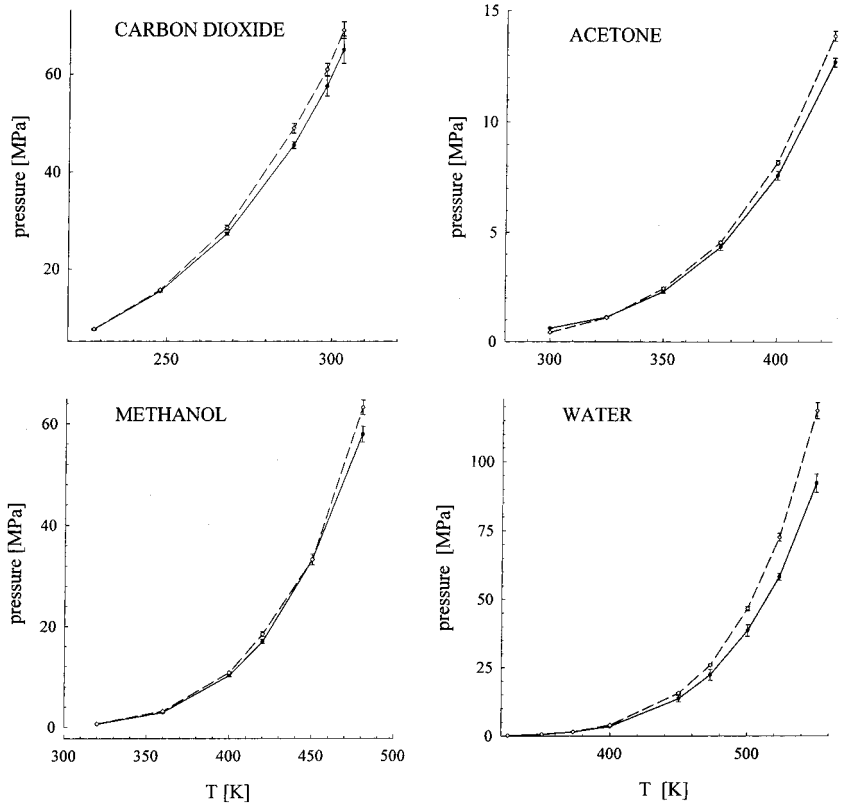

Figure 6. Comparison of orthobaric pressures of the full and short-range versions of the considered compounds. For the symbols see the caption for Figure 4.

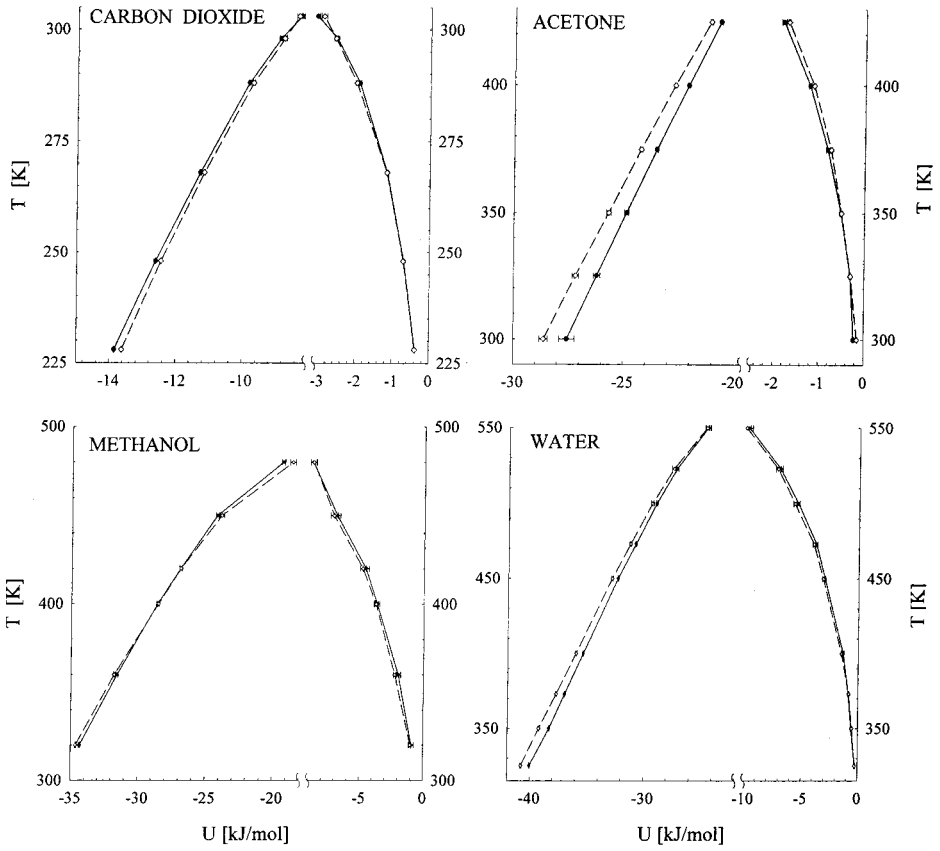

Figure 7. The same as Figure 6 for the internal energy.

agreement between U_{full} and U_{short} with increasing temperature (decreasing coexistence densities). Since the intermolecular interactions in acetone are, qualitatively, the same as in water, it is not surprising that the same behavior is also found for them. On the contrary, molecules of carbon dioxide do not form either hydrogen bonds or interact via dipole−dipole interaction and

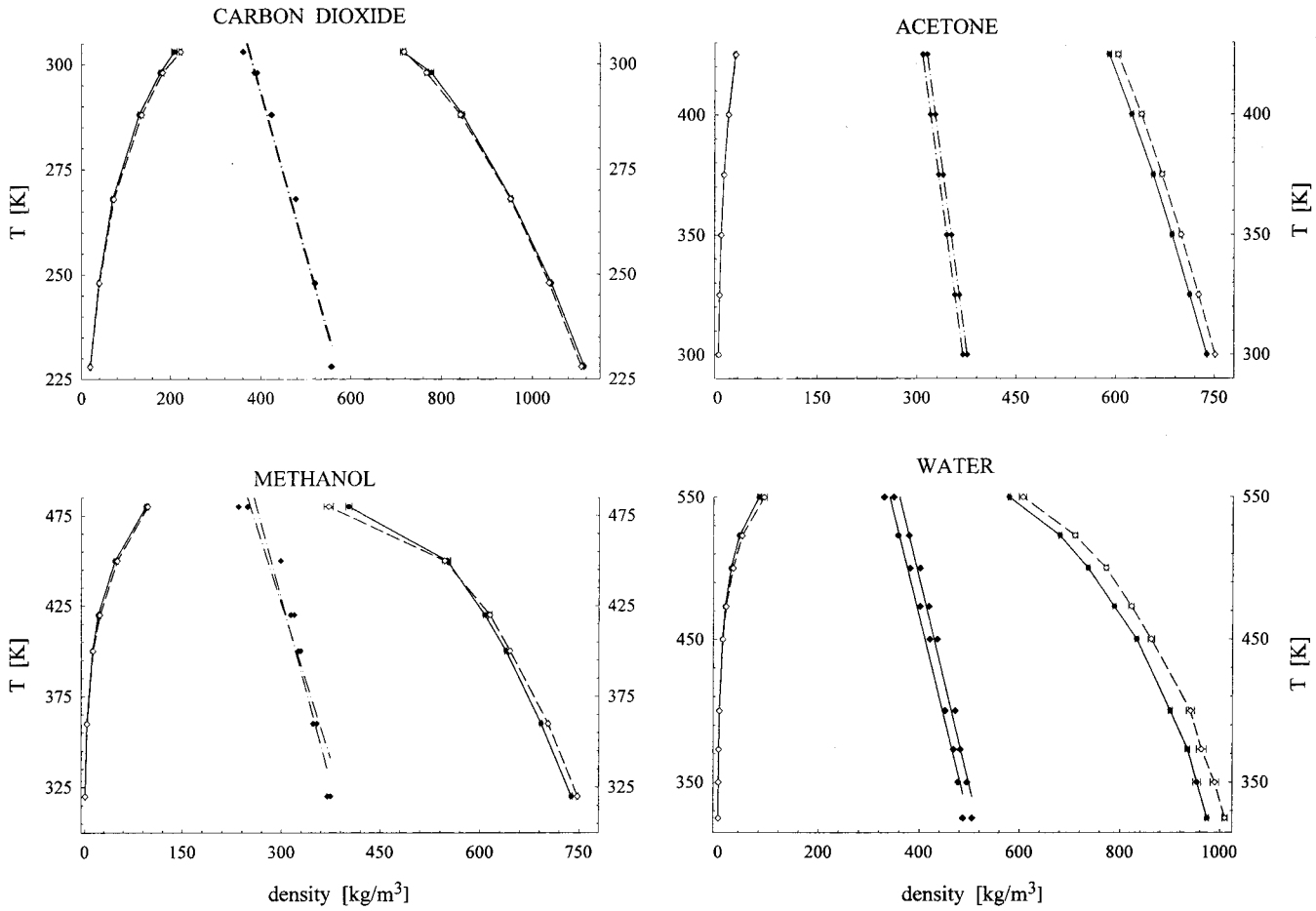

Figure 8. The same as Figure 6 for the coexistence densities. The straight lines correspond to the rectilinear diameter rule given by the fit according to eq 10.

this may be an explanation of its different temperature dependence of the internal energy. As regards methanol, the dependence of U along the coexistence curve is the same as that in the homogeneous phase, although the intermolecular interactions are qualitatively the same as for water: hydrogen bonding at short separations and strong dipole−dipole interaction at large separations. These differences only show that the details of the behavior of the fluids considered seems quite sensitive to details of the intermolecular interactions and that any intuitive predictions must be made with caution.

The coexistence envelope T vs ρ is shown in Figure 8. We see that for carbon dioxide and methanol there is only a marginal difference in the behavior of the short-range and full models. Discrepancies exceeding the combined simulation errors are found for liquid densities of acetone and water. For both these compounds the densities of the short-range model are greater than those of the full models which is consistent with higher pressure in the former systems. From the practical point of view an important problem is how these differences affect the location of the critical point. In the vicinity of the critical point the coexistence envelope can be expanded in the form[28]

$$\rho_l - \rho_v = A_0\Delta T^{\beta} + A_1\Delta T^{\beta+\Delta} + A_2\Delta T^{\beta+2\Delta} + ... \quad (8)$$

where $\Delta T = |\ 1 - T/T_c|$, T_c is the critical temperature, A_i are the amplitude coefficients, β is the critical exponent, and Δ is the so-called gap exponent. This equation can be used to estimate, by regression of experimental data, the critical temperature and the exponent β. To estimate the location of the critical density ρ_c, we need to use the corresponding equation

TABLE 3: Location of the Critical Point of the Short-range and Full Models, and Their Effective Critical Exponents as Estimated from the Wegner Expansion, Equation 10

	short-range		full			
	T_c	ρ_c	T_c	ρ_c	β_e^{short}	β_e^{full}
carbon dioxide	310.8	458.6	310.9	455.1	0.336	0.328
acetone	505.4	275.3	498.9	273.2	0.281	0.266
methanol	483.2	256.4	484.6	261.9	0.255	0.245
water	543.7	362.2	543.6	343.6	0.200	0.200

for the coexistence curve diameter, i.e.,

$$\frac{\rho_l + \rho_g}{2} = \rho_c + B_1\Delta T^{\phi} + B_2\Delta T + B_3\Delta T^{\phi+\Delta} + ... \quad (9)$$

Following the common practice (see, e.g., refs 29 and 30), the coefficients B_1 and B_3, A_1, and higher order coefficients are set to zero which yields the working equation

$$\rho_{\pm} = \rho_c + B_2\Delta T \pm \frac{1}{2}A_0\Delta T^{\beta_e} \quad (10)$$

where the plus sign refers to the liquid phase and the minus sign to the vapor phase, and subscript "e" at β indicates that the exponent is considered as an effective quantity. Using the least-squares method, we are now able to determine the critical density, the critical temperature, and the effective critical exponent. Results of this procedure are given in Table 3 and allow us to state the following: the long-range contributions to the intermolecular interactions have negligibly small or (practically) even null effect on the values of the critical conditions.

The critical temperatures for the short- and full-range models agree within the experimental errors for all compounds but acetone for which the difference slightly exceeds 1%. Practically the same agreement is found for the critical densities of carbon dioxide and acetone, whereas for the two associating compounds the difference is somewhat larger. The effective exponent β_e is only a mathematical quantity and it is hard to draw some physically meaningful conclusions with the exception that β_e for the full models is never greater than β_e for the short-range model. It is also important to note that β_e will approach the asymptotic value of β as ΔT goes to zero, with a slope that is fluid-specific (see, e.g., Figure 1 of ref 31). Thus, if this slope is very small, the effective and asymptotic values of β will be very close to each other. This is precisely the case of real carbon dioxide[31] and thus it is not surprising to find that the model of carbon dioxide used here predicts a very close estimate of the actual asymptotic β. However, other compounds exhibit negative slopes, and therefore, the temperature regression of the difference of orthobaric densities will predict a temperature-dependent slope, such that, the farther from the critical point we regress, the smaller the resulting effective exponent β_e. This behavior is consistent with our findings for methanol, water, and acetone (see Table 3).

In light of frequently found statements on the effect of the long-range forces on the critical conditions, the findings of Table 3 may appear to be at odds. The problem is that the effect of the multipole interactions cannot be assessed correctly using real experimental data only. To be more specific, unlike the electric charge, neither the dipole nor quadrupole moments are real quantities existing in nature. They result from the concept of estimating the electric field of a set of *charges* outside an enveloping sphere. The field outside molecules may be estimated by dipoles but at larger distances only and greater dipole/quadrupole only means greater partial charges or/and greater asymmetry in their distribution within the molecule. At close vicinity of the charge distribution the expansion in multipoles converges slowly and higher multipoles must therefore also be accounted for. From the complete neglect of the dipole−dipole interaction one may thus hardly draw any meaningful conclusions. In the short-range model defined by eq 5 the electrostatic interactions, and hence also the dipole−dipole interaction, are neglected only from certain separations onward where the dipole−dipole interaction dominates, whereas at short separations the electric field remains intact. Thus, the comparison of the properties of the short-range and full models is a way to assess properly the effect of the dipole−dipole interaction; however, these results cannot be compared with those mentioned earlier or with experimental data.

3.3. Interpretation of Results. We have discussed the results and made certain conclusions for four selected compounds. For methanol, the intuitive speculation on the pressure for the short-range and full systems is in agreement with the simulation results but for water much more complex dependence was found.[10] The question is thus whether the results may be interpreted in a general theoretical way which would make it possible to extend the conclusions to a wider spectrum of substances.

Let us start with the isothermal density dependence or isochoric temperature dependence of the effects of the long-range contributions to the intermolecular potentials on the system pressure and configurational internal energy. To that end we start by writing the total differential of the Helmholtz free energy of a pure fluid as a function of the absolute temperature, total volume, and a coupling parameter λ,[32] i.e.,

$$dA = -S\,dT - P\,dV + \left(\frac{\partial A}{\partial \lambda}\right)_{T,V} d\lambda \tag{11}$$

For convenience we define the coupling parameter so as to provide a bridge between the short- and long-range contributions to the intermolecular interactions,

$$U(\lambda) = U_{short} + \lambda U_{pert} \tag{12}$$

where $U(\lambda = 1) = U_{full}$. Making use of the basic statistical−mechanical relationships, the third term of eq 11 may be expressed as

$$\left(\frac{\partial A}{\partial \lambda}\right)_{V,T} = \langle U_{pert}\rangle = N u_p \tag{13}$$

where u_p is an average contribution per particle of the perturbation interaction to the configurational energy. Furthermore,

$$\left(\frac{\partial^2 A}{\partial V \partial \lambda}\right)_T = -\left(\frac{\partial P}{\partial \lambda}\right)_{V,T} = -N\left(\frac{\partial u_p}{\partial V}\right)_T = \rho^2\left(\frac{\partial u_p}{\partial \rho}\right)_T \tag{14}$$

Thus,

$$P_{full}(T,\rho) = P_{short}(T,\rho) + \int_0^1 \rho^2\left(\frac{\partial u_p}{\partial \rho}\right)_T d\lambda$$

$$\cong P_{short}(T,\rho) + \rho^2\left(\frac{\partial u_p}{\partial \rho}\right)_T \tag{15}$$

which means that the contribution of the long-range interactions can be estimated in terms of the density dependence of the average perturbation contribution to the configurational energy $\langle U_{pert}\rangle$, $\langle U_{pert}\rangle = \langle U_{full}\rangle - \langle U_{short}\rangle$.

Examination of Figure 5 gives for the perturbation contribution $(\partial u_p/\partial \rho)_T < 0$ which implies, according to eq 15, that the pressure in the full system must drop down and this is the case as seen also in Figure 5. Equation 15 makes it also possible to understand and explain a rather complex relation between pressure in the short- and full-range systems for water, see Table 3 of ref 10. For $T = 353$ K we have $P_{full} > P_{short}$, whereas for $T = 700$ K the opposite inequality holds true. Examination of the density dependence of the perturbation contribution to U shows that for $T = 353$ K we do have $(\partial u_p/\partial \rho)_T > 0$ and thus, according to eq 15 above, $P_{full} > P_{short}$. At the supercritical temperature $T = 700$ K the configurational energy of full water is smaller than that of short-range water and $(\partial u_p/\partial \rho)_T < 0$ which results in the reverse relation between pressures.

Now let us focus on the effect of the range on the coexistence pressure. For that purpose we follow a similar coupling parameter analysis, now based on the Gibbs free energy of both phases in equilibrium, i.e.,

$$dG^l = -S^l\,dT + V^l\,dP + (\partial G^l/\partial \lambda)_{T,P}\,d\lambda$$

$$dG^v = -S^v\,dT + V^v\,dP + (\partial G^v/\partial \lambda)_{T,P}\,d\lambda \tag{16}$$

After recalling the connection between $G(P, T, \lambda)$ and the configurational partition function we obtain, similarly to eq 13,

$$(\partial G^\alpha/\partial \lambda)_{T,P} = N u_p^\alpha \tag{17}$$

where the superscript refers to phases. Thus, from eqs 16 and

17 we obtain

$$-(S^{l} - S^{v})dT + (V^{l} - V^{v})\,dP = -N(u_p^{l} - u_p^{v})\,d\lambda \quad (18)$$

and, consequently, can write down the corresponding Clausius−Clapeyron-type equation in terms of the coupling parameter, i.e.,

$$\left(\frac{dP}{d\lambda}\right)_{\sigma,T} = -\frac{N(u_p^{l} - u_p^{v})}{(V^{l} - V^{v})} \quad (19)$$

where σ indicates phase coexistence conditions. Typically, $|u_p^{l}| \gg |u_p^{v}|$ and $V^{l} \ll V^{v} \approx NkT/P$ and then eq 19 becomes

$$\left(\frac{dP}{d\lambda}\right)_{\sigma,T} = -\frac{Nu_p^{l}}{V^{v}} \approx -\frac{P}{kT}u_p^{l} \quad (20)$$

whose integration leads to

$$P_{full} \cong P_{short}\exp(-u_p^{l}/kT) \quad (21)$$

The GEMC simulation results indicate that for water and acetone $|u_p^{l}| \gg |u_p^{v}|$, in addition to having $u_p^{l} > 0$, and therefore, according to eq 21, this behavior translates into $P_{full} < P_{short}$ as clearly observed in Figure 6. Methanol appears to be a special case in that $u_p^{l} \approx u_p^{v}$ holds true over the entire range of temperatures. Consequently, eq 19 cannot be reduced to the simplest form given by eq 21, and there is no clear-cut simplifying expression. Likewise, carbon dioxide is also an interesting case, in that the range of coexistence densities is much smaller than those for the other three systems, and therefore, the assumption $V^{l} \ll V^{v} \approx NkT/P$ does not apply. However, eq 19 can be reduced to

$$\left(\frac{dP}{d\lambda}\right)_{\sigma,T} \cong -\frac{Nu_p^{l}}{(V^{l} - V^{v})} \quad (22)$$

with $u_p^{l} < 0$ and $(V^{l} - V^{v}) < 0$, and therefore $P_{full} < P_{short}$ as observed in Figure 6.

An analysis of the orthobaric density dependence of the effects of the long-range contributions to the intermolecular potentials may proceed along the same line as above with the difference now on focusing on the chemical potential instead of on pressure. Thus, using again the coupling parameter and basic thermodynamic relationships, we may write

$$\mu_{full}^{l}(T, V^{l}) = \mu_{short}^{l}(T, V_{short}^{l}) + u_p^{l} \quad (23)$$

where u_p^{l} is the perturbation contribution in the liquid state. In addition, we can safely assume that in the vapor phase $\mu_{full}^{v}(T, V^{v}) \approx \mu_{short}^{v}(T, V_{short}^{v})$. By recalling now the condition of phase equilibrium we may write

$$\mu_{full}^{v}(T, V^{v}) = \mu_{full}^{l}(T, V^{l}) \cong \mu_{short}^{l}(T, V_{short}^{l}) + u_p^{l} \quad (24)$$

and hence,

$$\begin{aligned}\mu_{full}^{l}(T, V^{l}) - \mu_{full}^{v}(T, V^{v}) &= \int_{\rho^{v}}^{\rho^{l}} (d\mu_{full}/d\rho)_T d\rho \\ &= \int_{\rho^{v}}^{\rho^{l}} (P/\rho^2)d\rho = \int_{\rho^{v}}^{\rho_{short}^{l}} (P/\rho^2)d\rho + \int_{\rho_{short}^{l}}^{\rho^{l}} \underbrace{(P/\rho^2)}_{>0} d\rho \\ &= \Delta\mu_{short} + u_p^{l} \end{aligned} \quad (25)$$

where we have identified

$$\Delta\mu_{short} = \int_{\rho^{v}}^{\rho_{short}^{l}} (P/\rho^2)\,d\rho \quad (26)$$

and

$$u_p^{l} = \int_{\rho_{short}^{l}}^{\rho^{l}} \underbrace{(P/\rho^2)}_{>0} d\rho \quad (27)$$

From eq 27 we immediately see that u_p^{l} will have the same sign as $\rho^{l} - \rho_{short}^{l}$, and therefore this analysis suggests the following behavior:

$$u_p^{l} < 0 \Rightarrow \rho^{l} - \rho_{short}^{l} < 0 \Rightarrow U_{full}^{l} > U_{short}^{l}$$

such as that in the case of carbon dioxide;

$$u_p^{l} > 0 \Rightarrow \rho^{l} - \rho_{short}^{l} > 0 \Rightarrow U_{full}^{l} < U_{short}^{l}$$

such as that in the case of acetone and water; and

$$u_p^{l} \approx 0 \Rightarrow \rho^{l} - \rho_{short}^{l} \lesssim 0 \Rightarrow U_{full}^{l} \approx U_{short}^{l}$$

such as that in the case of methanol.

Note that methanol is not a clear-cut case in that $P_{full} \approx P_{short}$ and $U_{full}^{l} \approx U_{short}^{l}$ (within error bars).

4. Conclusions

The key to the understanding of fluid behavior hinges around the fact that different aspects of the intermolecular interactions, their range or origin or both, might be of relevance in different regions of the phase diagram. From very early we learned that in order to describe properly the thermodynamics of liquid-like fluids we needed to deal with models capable of predicting essentially the correct structure. Whereas the main finding for simple fluids has been that the fluid structure is primarily determined by the short-range repulsions, for polar and associating fluids the long-range electrostatic interactions have been claimed to be equally essential. Only recently has the latter claim been questioned and it has been shown that also in this case only the short-range part of these interactions may be relevant.

As a part of the ongoing investigation about the effect of the range of intermolecular interactions on the structural and thermophysical properties of polar and associating fluids, in this paper we have focused our attention on the predicted VLE behavior of four representative model fluids in terms of our proposed division into short- and long-range interactions. The main thrust of this analysis has been directed at shedding some light on the interplay between the strength and range of the interactions and their effect on the resulting behavior of coexisting phases.

The simulation results for the considered fluids confirm the previous findings for homogeneous phases, namely, that the properties of dense fluids are determined primarily by the short-range interactions regardless of their origin. As for the coexisting phases, although it seems that no particular general rule (of thumb) applies to the net effect on the orthobaric temperature−density and temperature−internal energy curves (orthobaric shifts), these effects can be unambiguously represented and interpreted by a simple perturbation approach in terms of the long-range contribution to the internal configurational energy of a short-range reference. These orthobaric shifts are practically zero for the vapor phase away from the fluid's critical point.

Most importantly, regardless of the type of orthobaric shift, the range of the model potential appears to have no effect on the fluid's critical conditions.

Our findings have interesting implications in the development of equations of state for fluids involving long-range interactions: i.e., contrary to the usual practice,[33−35] there is no need to invoke specific short- and long-range interactions in order to describe fluid behavior properly. Our general split into short- and long-range interactions fits naturally the format for a fast converging perturbation expansion approach to equations of state, one in which we can identify each resulting contribution and assign it a true molecular meaning.[12] In addition, these results also highlight the need for (i) an accurate description of the short-range contributions to the structure (and consequently the properties) of the fluid: i.e., the short-range reference fluid required in the perturbation approach,[36] and (ii) an investigation of fluids with an extreme strength of interactions, such as, e.g., hydrogen fluoride, to find limits of validity (if there are any) of the so far reached conclusions.

Acknowledgment. This research was supported by the Grant Agency of the Academy of Sciences of the Czech Republic (Grant A4072908/99), and by the Division of Chemical Sciences, Geosciences, and Biosciences, Office of Basic Energy Sciences, under contract number DE-AC05-00OR22725 with Oak Ridge National Laboratory, managed and operated by UT-Battelle, LLC. P.T.C. was supported by the Division of Chemical Sciences, Geosciences, and Biosciences, Office of Basic Energy Sciences, U.S. Department of Energy.

References and Notes

(1) Barker, J. A.; Henderson, D. *Rev. Mod. Phys.* **1976**, *48*, 587−671.
(2) Gray, C. G.; Gubbins, K. E. *Theory of Molecular Fluids*; Clarendon Press: Oxford, 1984.
(3) Waisman, E.; Lebowitz, J. L. *J. Chem. Phys.* **1970**, *52*, 4307−4309.
(4) Wertheim, M. S. *J. Chem. Phys.* **1971**, *55*, 4291−4298.
(5) Blum, L.; Wei, D. Q. *J. Chem. Phys.* **1987**, *87*, 555−565.
(6) Lee, L. L. *Molecular Thermodynamics of Nonideal Fluids*; Butterworth: Stoneham, 1988.
(7) Nezbeda, I.; Kolafa, J. *Czech. J. Phys.* **1990**, *B40*, 138−150.
(8) Nezbeda, I.; Kolafa, J. *Mol. Phys.* **1999**, *97*, 1105−1116.
(9) Kolafa, J.; Nezbeda, I. *Mol. Phys.* **2000**, *98*, 1505−1520.
(10) Nezbeda, I.; Lısal, M. *Mol. Phys.* **2001**, *99*, 291−300.
(11) Kolafa, J.; Nezbeda, I.; Lısal, M. *Mol. Phys.* **2001**, *99*, 1751−1764.
(12) Nezbeda, I.; Weingerl, U. *Mol. Phys.* **2001**, *99*, 1595−1606.
(13) Benavides, A. L.; Guevara, Y.; Del Rıo, F. *Phys. A* **1994**, *202*, 420−437.
(14) Prausnitz, J. M.; Lichtenthaler, R. N.; et al. *Molecular Thermodynamics of Fluid Phase Equilibria*; Prentice Hall: Englewood Cliffs, 1986.
(15) Jorgensen, W. I.; Chandrasekhar, J.; Madura, J. D.; Impey, R. W.; Klein, M. L. *J. Chem. Phys.* **1983**, *79*, 926−935.
(16) Jorgensen, W. L. *J. Phys. Chem.* **1986**, *90*, 1276−1284.
(17) Jedlovszky, P.; Pálinkás, G. *Mol. Phys.* **1995**, *84*, 217−233.
(18) Harris, J. C.; Yung, K. H. *J. Phys. Chem.* **1995**, *99*, 12021−12024.
(19) Frenkel, D.; Smit, B. *Understanding Molecular Simulation: From Algorithms to Applications*; Academic Press: San Diego, 1996.
(20) Cracknell, R. F.; Nicholson, D.; Parsonage N. G.; Evans, H. *Mol. Phys.* **1990**, *71*, 931−943.
(21) Flyvbjerg, H.; Petersen, H. G. *J. Chem. Phys.* **1989**, *91*, 461−466.
(22) Neumann, M. *Mol. Phys.* **1983**, *50*, 841−853.
(23) Nosé, S. *Mol. Phys.* **1984**, *52*, 255−268.
(24) Gear, C. W. *The Numerical Integration of Ordinary Differential Equations of Various Orders*; Argonne National Laboratory: Chicago, 1966.
(25) Evans, D. J.; Murad, S. *Mol. Phys.* **1977**, *34*, 327−331.
(26) Lısal, M.; Smith, W. R.; Nezbeda, I. *J. Phys. Chem. B* **1999**, *103*, 10496−10505.
(27) Table D-3 of ref 2.
(28) Wegner, F. J. *Phys. Rev. B* **1972**, *5*, 4529−4536.
(29) Green, D. G.; Jackson, G. *J. Chem. Phys.* **1994**, *101*, 3190−3204.
(30) Vega, L.; de Miguel. E.; Jackson, G. *J. Chem. Phys.* **1992**, *96*, 2296−2305.
(31) Singh, R. R.; Pitzer, K. S. *J. Chem. Phys.* **1989**, *90*, 5742−5748.
(32) Kirkwood, J. G. *J. Chem. Phys.* **1935**, *3*, 300−313.
(33) Fürst, W.; Renon, H. *AICHE J.* **1993**, *39*, 335−343.
(34) Jin, G.; Donohoue, M. *Ind. Eng. Chem. Res.* **1988**, *27*, 1073−1084.
(35) Zuo, J. Y.; Zhang, D.; Fürst, W. *AICHE J.* **2000**, *46*, 2318−2329.
(36) Mulero, A.; Galan, C.; Cuadros, F. *PCCP* **2001**, *3*, 4991−4999.